

AAV-Mediated *TAZ* Gene Replacement Restores Mitochondrial and Cardioskeletal Function in Barth Syndrome

Silveli Suzuki-Hatano,¹ Madhurima Saha,¹ Skylar A. Rizzo,¹ Rachael L. Witko,¹ Bennett J. Gosiker,¹ Manashwi Ramanathan,¹ Meghan S. Soustek,^{1,2} Michael D. Jones,¹ Peter B. Kang,^{1,2} Barry J. Byrne,^{1,2} W. Todd Cade,³ and Christina A. Pacak^{1,2,*}

Departments of ¹Pediatrics and ²Molecular Genetics and Microbiology, University of Florida College of Medicine, Gainesville, Florida; ³Program in Physical Therapy, Washington University School of Medicine, St. Louis, Missouri.

Barth syndrome (BTHS) is a rare mitochondrial disease that affects heart and skeletal muscle and has no curative treatment. It is caused by recessive mutations in the X-linked gene *TAZ*, which encodes tafazzin. To develop a clinically relevant gene therapy to restore tafazzin function and treat BTHS, three different adeno-associated virus serotype 9 vectors were tested and compared to identify the optimal promoter—cytomegalovirus (CMV), desmin (Des), or a native tafazzin promoter (Taz)—for *TAZ* expression following intravenous administration of 1×10^{13} vector genomes/kilogram to a mouse model of BTHS as either neonates (1–2 days of age) or adults (3 months of age). At 5 months of age, evaluations of biodistribution and *TAZ* expression levels, mouse activity assessments, fatigue in response to exercise, muscle strength, cardiac function, mitochondrial structure, oxygen consumption, and electron transport chain complex activity assays were performed to measure the extent of improvement in treated mice. Each promoter was scored for significant improvement over untreated control mice and significant improvement compared with the other two promoters for every measurement and within each age of administration. All three of the promoters resulted in significant improvements in a majority of the assessments compared with untreated BTHS controls. When scored for overall effectiveness as a gene therapy, the Des promoter was found to provide improvement in the most assessments, followed by the CMV promoter, and finally Taz regardless of injection age. This study provides substantial support for translation of an adeno-associated virus serotype 9-mediated *TAZ* gene replacement strategy using a Des promoter for human BTHS patients in the clinic.

Keywords: cardiac gene therapy, mitochondrial disease, AAV9, tafazzin, Barth syndrome, promoter comparison

INTRODUCTION

BARTH SYNDROME (BTHS) is a rare, frequently fatal, mitochondrial disease caused by recessive loss-of-function mutations in the X-linked gene *TAZ*, which encodes tafazzin. Tafazzin is a nuclear-encoded acyltransferase that is trafficked to the inner mitochondrial membrane. Under normal conditions, cardiolipin (CL) becomes degraded to monolysocardiolipin (MLCL) and is then converted back to mature CL by tafazzin. However, in BTHS this cycle is impaired and the accumulation of MLCL eventually leads to increased MLCL/CL ratios.^{1–5} The unique composition of mature CL is responsible for maintenance of mitochondrial membrane fluidity,

osmotic stability, and proper curvature of the cristae, which serves as a crucial binding site for electron transport chain (ETC) proteins and stabilization of the ETC supercomplexes.^{6–9} In BTHS mitochondria, the increased MLCL/CL ratios result in abnormal cristae formation and inefficient ETC-mediated ATP production.

The timing and clinical presentation of BTHS is variable; however, typical symptoms include cardioskeletal myopathy, neutropenia, and 3-methylglutaconic aciduria, with cardiomyopathy being the primary cause of death.^{10–13} Impaired cardiac and skeletal muscle bioenergetics, decreased cardiac reserve, and diminished skeletal

* Correspondence: Dr. Christina A. Pacak, Department of Pediatrics, University of Florida College of Medicine, 1200 Newell Drive, RG-183A, Gainesville, FL 32610. E-mail: pacakc@peds.ufl.edu

muscle O₂ utilization all contribute to an overall phenotype of cardioskeletal myopathy.^{11,13} Current clinical BTHS standard of care includes administration of medications such as diuretics and ACE inhibitors; no other treatment options are available for these patients.¹⁰ Recessive single-gene defect disorders such as BTHS are optimal targets for gene replacement strategies. The potential for various gene delivery systems to correct *TAZ* deficiency has been demonstrated in *Saccharomyces cerevisiae*, *Drosophila melanogaster*, *Danio rerio*, and *in vitro* iPSC BTHS models.^{5,14–16} In all of these, replacement of *TAZ* demonstrated improvement in the BTHS disease phenotypes (motor weakness, mitochondrial respiration, *in vitro* cardiomyocyte contractile function). In sum, these studies strongly support development of a clinically relevant gene therapy approach to treat BTHS.

Recombinant adeno-associated virus (rAAV) vectors are ideally suited for gene therapy approaches because the rAAV used for gene delivery is a non-pathogenic virus (with all viral genes removed) that elicits a minimal immune response and rAAV persists for long periods of time as an episome within the nucleus of cells providing stable gene transfer without disruption of genes by insertional mutagenesis.¹⁷ Employing several layers of vector optimization reduces the minimal effective dose and ultimately lowers both the cost of the therapeutic as well as the risk of side effects for patients. Identification of an ideal tissue restrictive promoter for use in a gene delivery system is one layer of optimization that we test in this study; another is the use of specific serotypes. Many laboratories performing independent AAV serotype comparison studies have concluded that AAV serotype 9 (AAV9) is the most naturally cardiotropic serotype available to date.^{18–22} In addition to a high affinity for the heart, intravenous administration of AAV9 has also been shown to provide exceptional transduction of skeletal muscle.^{18,19,22,23}

Here we describe a study designed to test and compare three different AAV2/9-*TAZ* vectors that each contain a different promoter to drive *TAZ* expression. One is a ubiquitous cytomegalovirus (CMV) promoter, another is a desmin (Des) promoter that is expected to provide high expression in heart and skeletal muscle and lower expression in nonmuscle, nonheart tissues such as liver, and the final promoter is the native *Taz* promoter, which is expected to provide more natural *TAZ* expression levels across all tissues. Our goal was to identify which promoter was the most effective at improving BTHS pathophysiology at each injection age. Assessments included evaluations of *TAZ* expression levels and biodistribution, mouse activity as-

sessments, fatigue in response to exercise, muscle strength, cardiac function, mitochondrial structure, oxygen consumption, and electron transport chain complex activity assays. Our data demonstrate successful correction of BTHS through significant organelle (mitochondria), organ (heart and skeletal muscle), and whole body functional improvements with all three promoters with Des being the most effective promoter regardless of injection age. In sum, we present preclinical data that provide strong support for further translation of BTHS gene therapy into the clinical realm.

MATERIALS AND METHODS

Tafazzin short hairpin RNA knockdown mice

The University of Florida Institutional Animal Care and Use Committee approved all animal studies. Wild type (WT) C57BL/6J female mice were mated to transgenic males (ROSA26 H1/^{TetO-shRNA:taz}) CB57BL/129S6 (previously characterized Tafazzin shRNA knockdown [TazKD] mouse model) for 5 days.^{24–28} Females were then separated from males and placed on a doxycycline (dox) diet containing 200 mg of dox/kg chow (TD98186; Envigo). Transgenic pups were identified by PCR genotyping of tail genomic DNA and maintained on the dox diet throughout their lives (TazKD). Nontransgenic WT littermates were also fed the dox diet and used as wild type controls in all experiments.

AAV vector design and administration

The promoter-*TAZ* sequences were cloned into a previously described double-stranded (ds) AAV plasmid sequence kindly provided by Dr. Xiao²⁹. Two of the plasmids contain the previously described desmin (Des) and CMV promoters and the other is *Taz*, a native tafazzin promoter, which contains the immediate 1071 bp sequence of the upstream 5' untranslated region of *TAZ*. Each promoter drives expression of the full-length human *TAZ* transgene complementary DNA (cDNA) (CCDS14748.1) tagged with a myc sequence and contains a poly-A tail. Each dsAAV plasmid was packaged into recombinant AAV9 capsids that were generated and titered at the University of Florida Vector Core facility in parallel using a *TAZ* probe and a well-established dot-bot method.³⁰ dsAAV9-CMV-*TAZ*, dsAAV9-Des-*TAZ*, and dsAAV9-*Taz*-*TAZ* were each administered to TazKD mice at a dose of 1×10^{13} vg/kg. Adult injections were administered through the jugular vein (at 3 months of age) and neonatal injections were administered through the superficial tem-

poral vein (at 1–2 days of age) as previously described.¹⁹ All *in vivo* assessments were performed at 5 months of age. Upon the completion *in vivo* experiments, mice were euthanized the same week and necropsies performed to enable force mechanics studies or mitochondrial oxygen consumption assays on freshly isolated tissues. Other tissues were collected and stored at -80°C until needed for other assays.

Vector genome assessments

A standard curve was generated by spiking in known quantities of *TAZ* plasmid into a background of negative control genomic DNA from wild type mice and performing quantitative PCR using a *TAZ* primer-probe. Genomic DNA was extracted from frozen tissues ($n = 3$ per tissue, per treatment cohort) using the Quick-DNA micro-prep kit (Zymo) and evaluated using the same *TAZ* primer-probe (45 ng of DNA per reaction). Vector genomes per diploid cell were calculated as previously described.^{19,31}

RT-PCR gene expression analyses

Total RNA was isolated from frozen tissues using the RNA Extraction kit (Zymo). cDNA was synthesized using the High Capacity RNA-to-cDNA kit (Applied Biosystems) and quantitative real-time (RT)-PCR was performed using TaqMan Master Mix (Thermo Scientific) and specific primers (Supplementary Table S1) (Thermo Scientific) on a StepOnePlus Real-Time PCR System (Applied Biosystems). Relative expression levels were calculated using the $\Delta\Delta\text{Ct}$ method to determine fold change as compared to control levels.

Protein quantification and Western blot analyses

Tissues were homogenized in RIPA lysis buffer containing protease and phosphatase inhibitors. Protein concentrations were determined using the DC Protein Assay kit (BioRad). Samples were resolved on 5–10% bis-tris polyacrylamide denaturing gels and transferred to nitrocellulose membranes using standard techniques. Membranes were incubated with primary antibodies (Supplementary Table S2) overnight at 4°C . Membranes were washed with $1\times$ Tris-buffered saline with Tween, incubated with secondary antibodies conjugated to horseradish peroxidase (1:1000) for 1 h, and washed again. Bands were detected using the Amersham ECL Prime Western Blotting Detection Reagent (GE Healthcare Life Science).

Myc pulldown assay

Tissues were homogenized in RIPA lysis buffer containing protease and phosphatase inhibitors. Protein lysate concentrations were determined using the DC Protein Assay kit (BioRad). One hundred micrograms of total protein were incubated for 16 h at 4°C with $100\ \mu\text{L}$ of Pierce Anti-c-Myc Agarose (Thermo Scientific), washed $3\times$ with Tris-buffered saline with 0.05% Tween-20 detergent and eluted from beads by boiling in Laemmli sample buffer.

Immunofluorescence microscopy

Freshly excised tissue samples were fixed in 10% neutral buffered formalin overnight at 4°C . Following fixation, tissues were embedded in paraffin and sectioned using standard methods. Slides were dried overnight at 37°C , dewaxed, rehydrated, and subjected to antigen retrieval using trypsin-EDTA. Slides were blocked in phosphate-buffered saline (PBS) +5% bovine serum albumin (BSA) for 1 h at room temperature then incubated in 1° antibodies (Supplementary Table S2) diluted in PBS +5% BSA overnight at 4°C . Following washes, slides were incubated in 2° antibodies diluted (1:200) + $1\ \mu\text{g}/\text{mL}$ 4',6-diamidino-2-phenylindole (Sigma Aldrich) in PBS +5% BSA for 1 h at room temperature. Slides were rinsed in $1\times$ PBS, mounted in VectaMount and stored at 4°C . Immunofluorescence (IF) images were acquired within 24 h of immunolabeling.

Activity and fatigue analyses

Rearing, distance, resting times, and mean velocity activities were evaluated in 5 month old mice using the ActiTrack v2.7 system (Panlab software) as previously described with slight modifications.^{32–34} Briefly, mice were placed in the detection chamber to assess total distance and vertical activity for 6 minutes prior to exercise. Next, the mice were mildly exercised on a treadmill (5 min at 3 m/min followed by an increase to 10 m/min for 10 min). Post-treadmill activity was then measured using the same method described for pre-treadmill activity. Zone map tracings were created using the Actitrack mapping software where the x and y planes represent the two dimensions of the activity chamber, and the bold lines represent every time the mouse breaks the z plane, registering as vertical activity within each 6 min time interval (pre- and postexercise). Each mouse was tested twice by blinded observation.

Echocardiography analyses

Five month old mice were anesthetized using a mixture of 1.5% isoflurane and O_2 . Acquisitions were obtained using the LOGIQ system and software

(GE Health Care). Long axis echocardiography (echo) measurements at the minor chord dimension were acquired in a standard long axis view. Short axis measurements were acquired on all mice at 5 months of age just below the midpapillary muscle. At least 10 consecutive beats of the left ventricular interior dimension (LVID) were recorded for both end diastole and end systole in each view. These measurements were averaged to calculate LVIDd (end diastolic) and overall fractional shortening for functional comparisons. The left ventricular posterior wall thickness was measured in end diastole for at least 10 consecutive beats and averaged.

Force mechanics

Soleus muscles were isolated from mice with the tendons attached and suspended vertically in a water-jacketed bath containing Krebs–Henseleit solution equilibrated with a 95% O₂/5% CO₂ gas mixture and maintained at 37°C. Solei were stimulated using two vertical platinum electrodes. Contractile properties were measured isometrically following determination of optimum length. Peak isometric tetanic force was measured at 160 Hz using a 500 ms train with a 2 min recovery period. Muscle fatigue was determined by measuring isometric contractile force stimulated by 250 ms, 30 Hz trains occurring every 4 s over a 5 min period. A force frequency relationship was determined by stimulating muscles to contract using a 500 ms train with a 2 min recovery period at the following frequencies: 15 Hz, 30 Hz, 60 Hz, 100 Hz, 160 Hz, and 200 Hz. Equipment included: Grass AC/DC Strain Gage Amplifier (model P122), Aurora Scientific Inc. Signal Interface, Grass S48 Stimulator, Grass Force Displacement Transducer (model FT03), ASI 610A Dynamic Muscle Control v5.420 software for data collection, and ASI 611A Dynamic Muscle Analysis v5.110 software.

Electron micrograph processing and analyses

Freshly excised 3 mm × 3 mm left ventricular wall heart tissue samples were placed in Karnovsky's fixative (2% paraformaldehyde/2.5% glutaraldehyde in 0.1 M sodium cacodylate buffer) and maintained at 4°C until processing. Tissue embedding, sectioning, and imaging were performed by the Emory University Robert P. Apkarian Integrated Electron Microscopy Core. All measurement analyses were performed by laboratory personnel blinded to sample identities using ImageJ software (National Institutes of Health).

Oxytherm analyses

Mitochondrial isolations were performed on fresh heart tissue as previously described.³⁵ Oxy-

gen consumption measurements were acquired by diluting samples (*n* = 5 per group) in 0.5 mL of respiration buffer (Mir05: 0.5 mM EGTA, 3 mM MgCl₂, 60 mM lactobionic acid, 20 mM taurine, 10 mM KH₂PO₄, 20 mM HEPES, 110 mM sucrose, 1 g/L BSA) in the chamber of an Oxytherm electrode unit (Hansatech, Norfolk, UK) at 37°C with constant stirring speed (60 rpm). The probe electrodes were calibrated with sodium dithionite (0% oxygen) and respiration buffer (100% oxygen) as recommended by the manufacturer. The measurements were acquired following additions of: 100 μL of isolated mitochondria, 10 μL substrate (0.25 M glutamate/0.125 M malate), 7.5 μL 10 mM adenosine 5'-diphosphate sodium salt (ADP) (state 3), 0.5 μL of oligomycin (5 mg/mL) (state 4_o), and 1 μL of 100 μM carbonyl cyanide 4-(trifluoromethoxy) phenylhydrazone (FCCP) (state 4_u).

ETC complex activity assays

All complex activity assays (CI, complex 1; CII, complex 2; and CIII, complex 3) were performed on homogenates of isolated cardiac mitochondria from mice at 5 months of age in triplicate (*n* = 5 per group) using a published protocol.³⁶ Briefly, CI activity was determined by oxidation of NADH to NAD at 340 nm using a SpectraMax i3x. Ten microliters of isolated mitochondrial homogenate was diluted into 90 μL of 50 mM phosphate buffer (pH 7.5), 100 μM NADH, 60 μM ubiquinone, 3 mg/mL fatty acid-free BSA, 300 μM potassium cyanide (KCN), and 10 μM rotenone (in parallel). CI activity was described as % inhibition following addition of rotenone. CII activity was determined by reduction of DCPIP (2,6-dichlorophenolindophenol sodium salt hydrate) at 600 nm. Ten microliters of isolated mitochondrial homogenate was diluted into 90 μL of 25 mM phosphate buffer (pH 7.5), 1 mg/mL fatty acid-free BSA, 300 μM KCN, 20 mM succinate, 50 μM decylubiquinone, 80 μM DCPIP, and 10 mM malonate (in parallel). CII activity was described as % inhibition following addition of malonate. CIII activity was measured as the conversion of oxidized cytochrome *c* to a reduced form at 550 nm. 10 μL of mitochondrial homogenate was diluted into 90 μL of 25 mM phosphate buffer (pH 7.5), 75 μM oxidized cytochrome *c*, 500 μM of KCN, 100 μM EDTA (pH 7.5), 0.025% (vol/vol) Tween-20, 100 μM of decylubiquinol and 10 μg/mL antimycin A (in parallel). CIII activity was described as % inhibition following addition antimycin A.

Statistical analyses

Data were analyzed for significance using SPSS Software. Values are reported as mean ± standard

error. Significant differences were determined by nonparametric Kruskal Wallis and Dunn post-hoc tests. Differences between promoter groups from the same age of injection are indicated by an asterisk (*) and lines above bars. Significant improvement between each cohort and untreated TazKD controls are indicated by an asterisk (*) at the bottom of bars ($*p \leq 0.05$, $**p \leq 0.01$, $***p \leq 0.001$ were considered statistically significant).

RESULTS

CMV, Des, and Taz promoters provide differential TAZ expression profiles *in vivo*

Recombinant AAV includes two flanking palindromic inverted terminal repeats that are essential for virus replication and for packaging into cap-

sids³⁷. In order to develop the optimal gene delivery vector for BTHS, we created three different TAZ expression cassettes flanked by inverted terminal repeats designed to efficiently generate double-stranded (dsAAV) vectors (Fig. 1A).²⁹ One contains a CMV promoter to provide robust, long-term TAZ expression in a wide variety of tissues. Another contains a previously described desmin promoter (Des) that has been shown to drive efficient transgene expression in striated (heart and skeletal) muscle.^{23,38} We also evaluated the ability of the 5' untranslated region of TAZ to serve as an efficient promoter (Taz). This region contains multiple promoter-like elements including 14 different transcription factor binding sites. Each cassette also contains a poly-A tail. All three were packaged into AAV serotype 9 (AAV9) capsids due to this

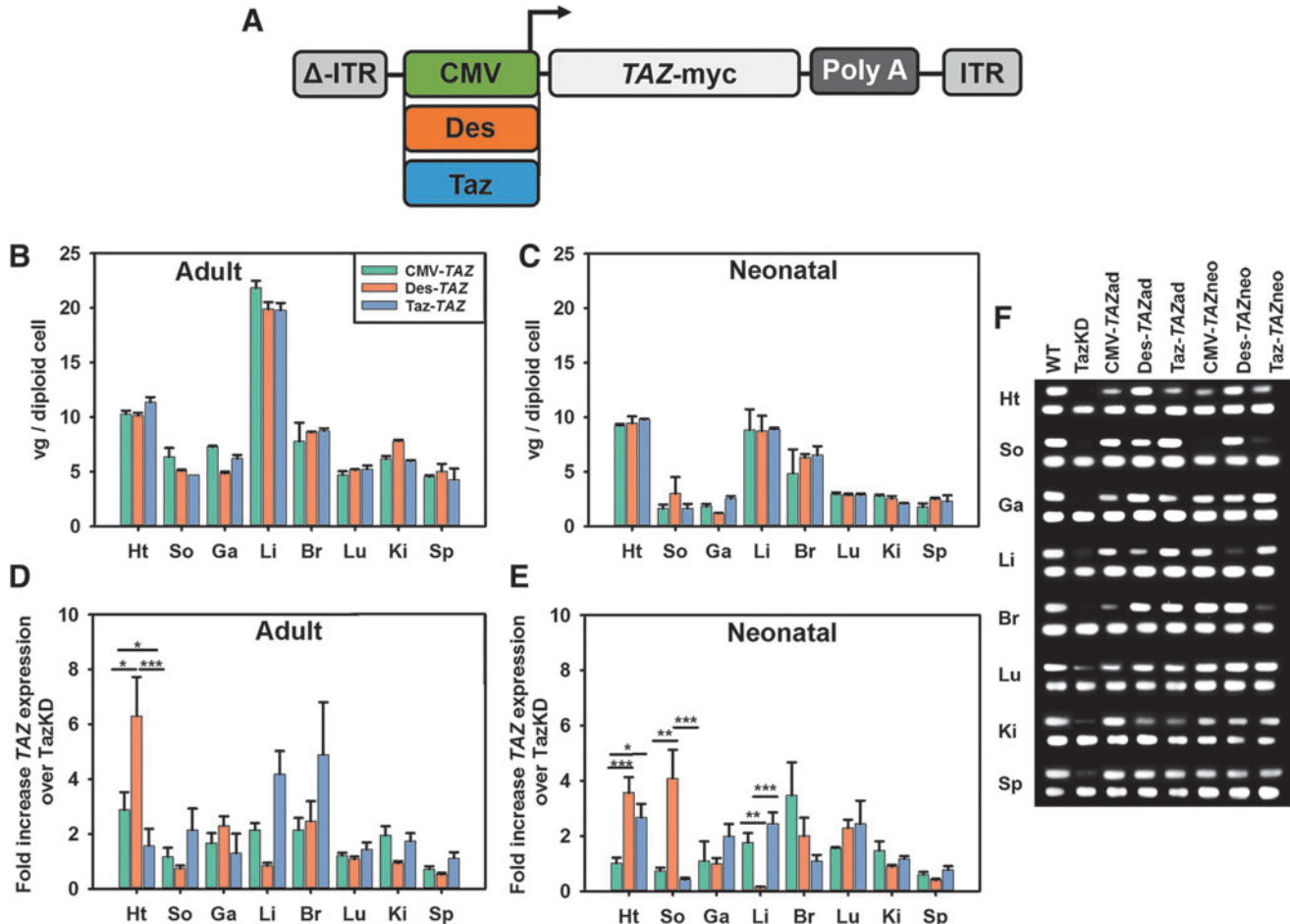


Figure 1. AAV-TAZ vector designs and RNA transcription levels. **(A)** Depiction of the three different TAZ-myc + Poly A tail constructs, each containing a different promoter and flanked by AAV-ITRs mutated to form double-stranded vectors (indicated by Δ). No significant difference between promoters was observed in vector genomes (vg) per diploid cell across tissues from mice treated as adults (3 months of age) **(B)** or as neonates (1–2 days of age) **(C)**. Human TAZ RNA transcript expression levels were evaluated in tissues from mice injected as adults **(D)** and neonates **(E)**. **(F)** Gel showing representative bands for each tissue generated with TAZ (top) and 18S (bottom) gene expression probes for each sample. Data are represented as mean \pm SEM ($n=6$). Significant differences between promoters were determined using the Kruskal–Wallis test ($*p \leq 0.05$, $**p \leq 0.01$, $***p \leq 0.001$). ad, adult; AAV, adeno-associated virus; Br, brain; CMV, cytomegalovirus; Des, desmin; Ga, gastrocnemius; Ht, heart; ITR, inverted terminal repeat; Ki, kidney; Li, liver; Lu, lung; neo, neonatal; So, Soleus; S, spleen; TazKD, tafazzin short hairpin RNA knockdown; WT, wild type.

serotype's high natural affinity for cardiac tissue following intravenous administration.¹⁹

TazKD mice were intravenously administered 1×10^{13} vector genomes/kilogram of dsAAV9-CMV-TAZ (CMV-TAZ), dsAAV9-Des-TAZ (Des-TAZ), or dsAAV9-Taz-TAZ (Taz-TAZ) as neonates (1–2 days of age; temporal vein) or adults (3 months of age; jugular vein). Following live functional assessments at 5 months, WT, untreated TazKD, and all six treated TazKD cohorts were euthanized for various tissue analyses. Vector genomes per diploid cell were determined for all tissues collected in this study (Fig. 1B and C). As expected, no differences in vector genomes were observed between promoters within the same tissue and injection age. These results confirm that the vector titers used were valid, the mice were administered uniform vector doses, and that any subsequent differences observed between mouse cohorts are a result of promoter effects.

Gene expression assays demonstrated that while all three vectors successfully transcribed TAZ, the different promoter sequences yielded varying TAZ transcript levels and tissue expression biodistributions that were slightly altered depending upon injection age. In the hearts of TazKD mice treated as adults, the Des-TAZ vector resulted in significantly higher TAZ gene expression levels than either CMV-TAZ or Taz-TAZ and the CMV-TAZ vector resulted in significantly higher TAZ gene expression levels than Taz-TAZ (Fig. 1D). No significant differences were observed between the three promoters in soleus, gastrocnemius, liver, brain, lung, kidney, or spleen from mice injected as adults. In the hearts of TazKD mice treated as neonates, both the Des-TAZ and Taz-TAZ vectors resulted in significantly higher TAZ gene expression levels than CMV-TAZ. The Des promoter also yielded significantly higher TAZ transcript levels in the soleus and significantly lower levels in liver as compared to both the CMV-TAZ and Taz-TAZ (Fig. 1E). There were no significant differences observed between expression levels from the different promoters in gastrocnemius, brain, lung, kidney, or spleen from mice treated as neonates. cDNA products from the gene expression assays were resolved on agarose gels and further confirmed these expression profile results (Fig. 1F).

Tafazzin protein expression was compared between the three promoters at both injection ages using Western blotting (WB) and IF microscopy on heart samples from each cohort. WB analysis with an α -tafazzin antibody shows bands at the correct size from whole heart lysate samples with the most intense bands coming from the Des-TAZ vector in mice injected as adults and lighter but prevalent

bands from all cohorts injected as neonates (Fig. 2A). WB analysis on whole heart lysate samples with an α -Myc antibody shows a band at the correct size with an intensity profile similar to α -tafazzin in samples treated as adults with Des-TAZ and more faintly in samples treated with each promoter as neonates. WB analysis with an α -Myc antibody on myc pulldown samples resulted in a band only from the Des-TAZ vector in mice injected as adults. Densitometry analyses of tafazzin/GAPDH protein band intensity ratio means from three separate whole heart lysate blots showed significantly higher levels of tafazzin protein present in hearts from Des-TAZ animals treated as adults as compared to CMV and Taz (Fig. 2B). IF microscopy was performed using (1) an antibody against the mitochondrially encoded cytochrome C oxidase II (MTCO2) protein to identify mitochondria (green) and (2) an α -Myc antibody (red) to detect protein expression from the delivered transgene (Fig. 2C–J). Myc expression was absent in both WT and TazKD controls (Fig. 2C and D) and detected by IF to some degree in all treated cohorts where it mimicked RNA transcript profiles and overlaid well with MTCO2 (Fig. 2E–J).

TAZ gene therapy improves whole body activity in TazKD mice

To simulate previous exercise-induced fatigue studies performed in human BTHS patients, mouse activities were evaluated prior to and following exercise using an ActiTrack system. WT, untreated TazKD, and all treated TazKD mice cohorts were evaluated in their average resting times (no movement), slow movement time, fast movement time (≥ 5 cm/s), total distance travelled, and number of vertical rearings prior to and immediately following 15 min of treadmill incline exercise. Preexercise resting time was significantly reduced in all treatment groups except Taz-TAZ mice treated as adults and there were no differences observed between promoters (Fig. 3A). Postexercise resting time was significantly reduced in all treatment groups except for Taz-TAZ mice treated as neonates with both the CMV-TAZ and Des-TAZ mice treated as neonates displaying significantly improved times as compared to Taz-TAZ mice (Fig. 3B). The average slow movement times preexercise were significantly improved in all treatment cohorts as compared to untreated controls except for CMV-TAZ mice treated as neonates with a significant difference between the CMV-TAZ and Taz-TAZ vectors in mice treated as adults (Fig. 3C). The average slow movement times postexercise were significantly improved in all treatment cohorts with mice

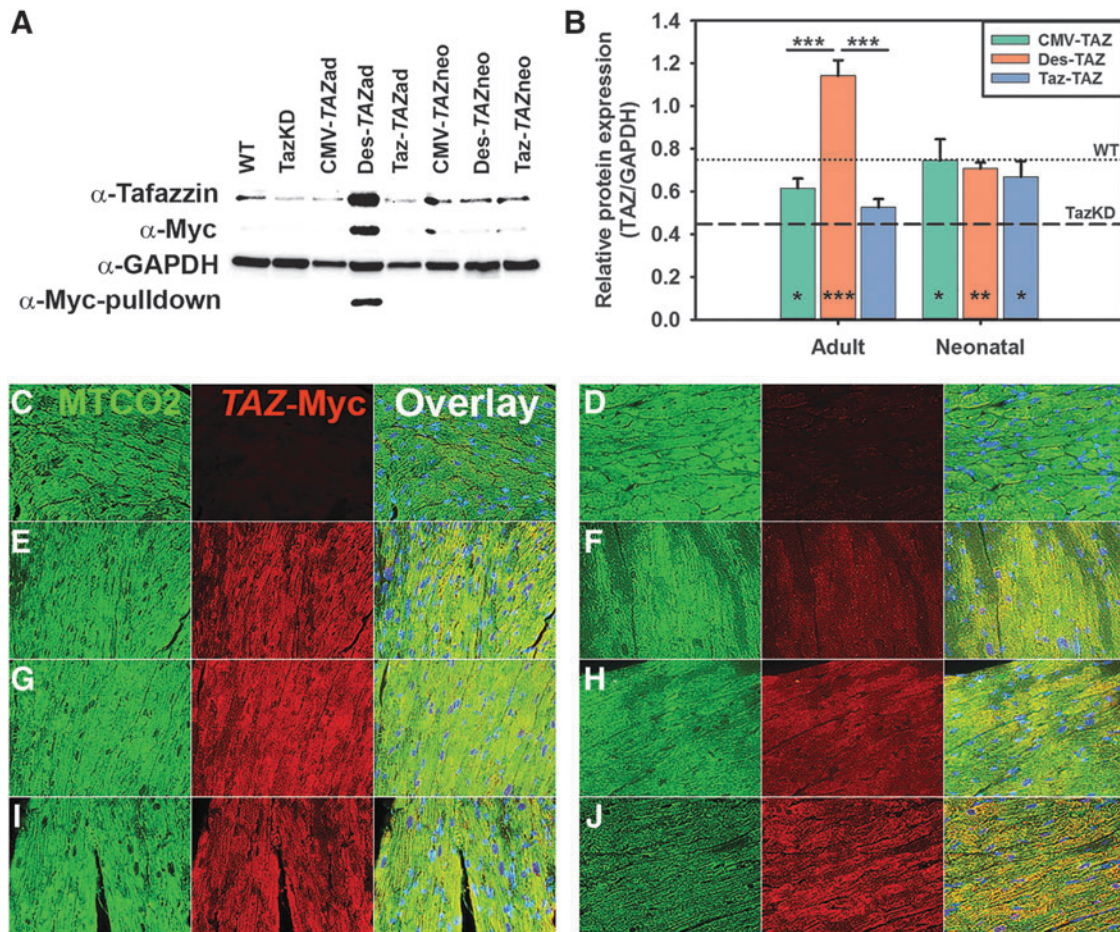


Figure 2. Tafazzin protein expression comparisons between AAV-TAZ vectors following delivery to adult or neonatal TazKD mice. **(A)** Representative Western blot analyses using (1) α -Myc antibody, (2) α -tafazzin antibody, (3) GAPDH control antibody on whole heart lysates, or (4) α -Myc antibody on Myc-bead purified (pull-down) heart lysate samples. **(B)** Graph depicting tafazzin/GAPDH Western blot density ratios for whole heart lysate samples. Data are represented as Mean \pm SEM ($n=3$ biological replicates). Significant differences between promoters for each treatment age are indicated by lines above bars and significant improvement between each individual sample and untreated TazKD controls is indicated at the bottom of bars (* $p \leq 0.05$, ** $p \leq 0.01$, *** $p \leq 0.001$). **(C–J)** Immunofluorescence analyses of the MTCO2 mitochondrial protein (left panel for each) and the Myc tag (middle panel for each) and an overlay of the two including DAPI in blue (right panel for each) shows no Myc expression in WT **(C)** or TazKD **(D)** mouse heart sections and varying levels of expression in hearts representing mice from all treatment cohorts: CMV-TAZad **(E)**; CMV-TAZneo **(F)**; Des-TAZad **(G)**; Des-TAZneo **(H)**; Taz-TAZad **(I)**; and Taz-TAZneo **(J)**.

treated with the Des-TAZ vector as neonates showing significantly more improvement as compared to the other two promoters (Fig. 3D).

Average fast movement time was significantly increased in all treatment groups as compared to untreated TazKD controls both preexercise (Fig. 3E) and postexercise (Fig. 3F). CMV-TAZ mice showed significant improvement over Taz-TAZ mice treated as adults preexercise and Des-TAZ mice showed significant improvement in postexercise fast movement time over both other promoters in mice treated as neonates with CMV-TAZ also showing significant improvement over Taz-TAZ mice treated as neonates. Preexercise total distance travelled was significantly increased in all treatment groups and no significant differences were observed between promoters (Fig. 3G). Postexercise total

distance travelled was also significantly increased in all treatment groups with Des-TAZ mice treated as neonates displaying significant improvement over both of the other promoters (Fig. 3H). The preexercise average number of rearings (number of times mice reach vertically and cross a horizontal plane) was significantly increased in all treatment groups over untreated TazKD mice with Des-TAZ mice treated as neonates showing significant improvement over both other promoters (Supplementary Fig. S1A). The postexercise average number of rearings was significantly increased in all treatment groups except for Taz-TAZ mice treated as adults and mice treated with Des-TAZ as neonates showed significant improvement over those treated with Taz-TAZ (Supplementary Fig. S1B).

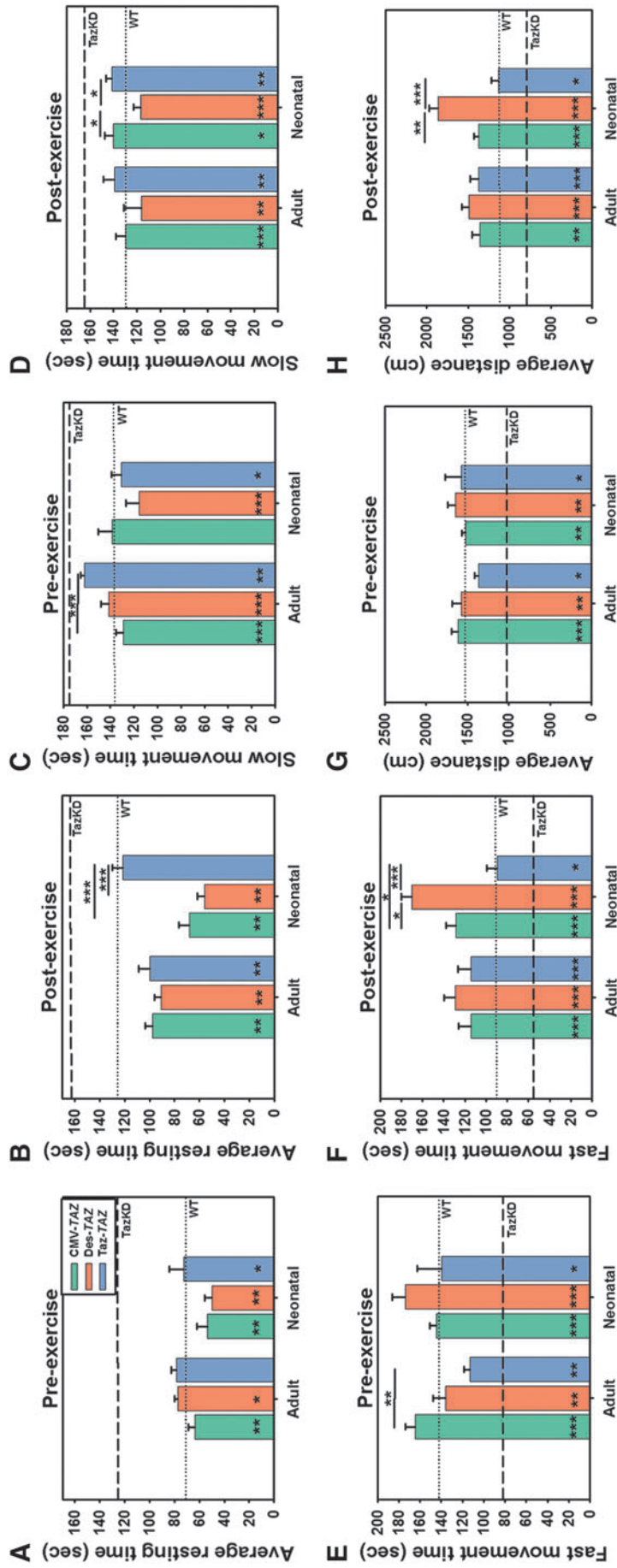


Figure 3. Mouse activity comparisons pre- and post-treadmill exercise. **(A)** A significant difference in pre-exercise resting time is observed between WT (dotted line) and TazKD (dashed line) but no significant difference is observed between the two post-exercise. **(B)** Average resting times are decreased in all treatment cohorts as compared to untreated TazKD controls pre- and post-exercise except for Taz-TAZ treated as adults (pre) and neonates (post). A significant difference in slow movement time is observed between WT and TazKD mice both pre-exercise **(C)** and post-exercise **(D)** ($p \leq 0.001$) and this is decreased in all treatment cohorts except CMV-TAZ treated as adults with differences between promoters indicated. **(E, F)** A significant decrease in fast movement time is observed in TazKD mice as compared with WT mice both pre- and post-exercise ($p \leq 0.01$) and this is significantly increased in all treatment cohorts. A significant decrease in average distance traveled is observed in TazKD mice as compared to WT controls both pre- and post-exercise ($p \leq 0.01$) and this is also increased in all treatment cohorts **(G, H)**. Data are represented as Mean \pm SEM ($n \geq 5$). Significant differences between promoters for each treatment age are indicated by lines above bars and significant improvement between each individual sample and untreated TazKD controls is indicated at the bottom of bars (* $p \leq 0.05$, ** $p \leq 0.01$, *** $p \leq 0.001$).

Activity maps generated for each mouse pre and post exercise further demonstrate the impact of tafazzin deficiency on overall movement. WT and treated TazKD mice were able to more quickly assess their environment and better explore territory within the arena (Supplementary Fig. S2A–D and F–H). As untreated TazKD mice spent more time resting or moving slowly, it took longer for these mice to become comfortable with their surroundings and explore the center of the arena and thus, less of the arena area was explored (Supplementary Fig. S2E). Of note, among treatment groups, mice injected with the Taz-TAZ vector (although significantly improved over untreated TazKD controls) show the least improvement in movement type and territory coverage (Supplementary Fig. S2D and H). Taken together, ActiTrack data demonstrate significant improvements in body function and exercise tolerance in AAV treated TazKD mice as compared to untreated TazKD controls.

TAZ gene therapy improves cardiac function in TazKD mice

Echocardiography (echo) analyses were performed to compare cardiac function between all treatment cohorts at 5 months of age. All treatment

groups showed significant improvements in fractional shortening with Taz-TAZ mice showing significant improvement over CMV-TAZ and Des-TAZ vectors in mice treated as adults (Fig. 4A). All treatment groups showed significant improvements in ejection fraction with Taz-TAZ mice showing significant improvement over CMV-TAZ and Des-TAZ vectors in mice treated as adults (Fig. 4B). A table of the echo data used to generate these graphs is provided (Supplementary Table S3). Heart weight/body weight ratios were significantly improved in all treatment cohorts as compared to untreated TazKD controls except CMV-TAZ and Taz-TAZ treated as neonates with no differences observed between promoters (Fig. 4C).

Muscle force mechanics testing reveals differences in promoters' abilities to improve soleus muscle strength and fatigue

Ex vivo force mechanics evaluations were performed on excised soleus muscles from mice in all groups at five months of age. TazKD mice treated with either CMV-TAZ or Des-TAZ as neonates or adults all displayed a significant decrease in fatigability as compared to untreated TazKD controls

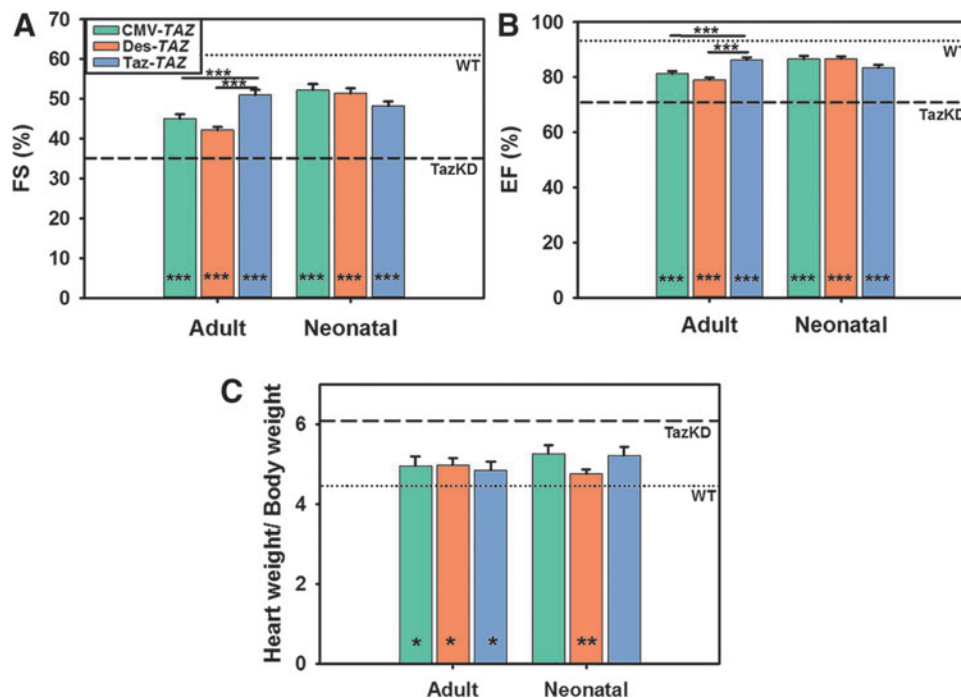


Figure 4. Cardiac function and heart weight characterizations. A significant decrease in FS% (A) and EF% (B) is observed in TazKD (dashed line) as compared to WT (dotted line) mice ($p \leq 0.001$). These measurements were both increased in all treated cohorts. (C) TazKD mice also display a significantly increased heart weight/body weight ratio as compared to WT controls ($p \leq 0.001$) that is decreased in all treated cohorts except CMV-TAZ and Taz-TAZ mice treated as neonates. Data are represented as mean \pm SEM ($n=8$). Significant differences between promoters for each treatment age are indicated by lines above bars and significant improvement between each individual sample and untreated TazKD controls is indicated by * at the bottom of bars (* $p \leq 0.05$, ** $p \leq 0.01$, *** $p \leq 0.001$). FS, fractional shortening; EF, ejection fraction.

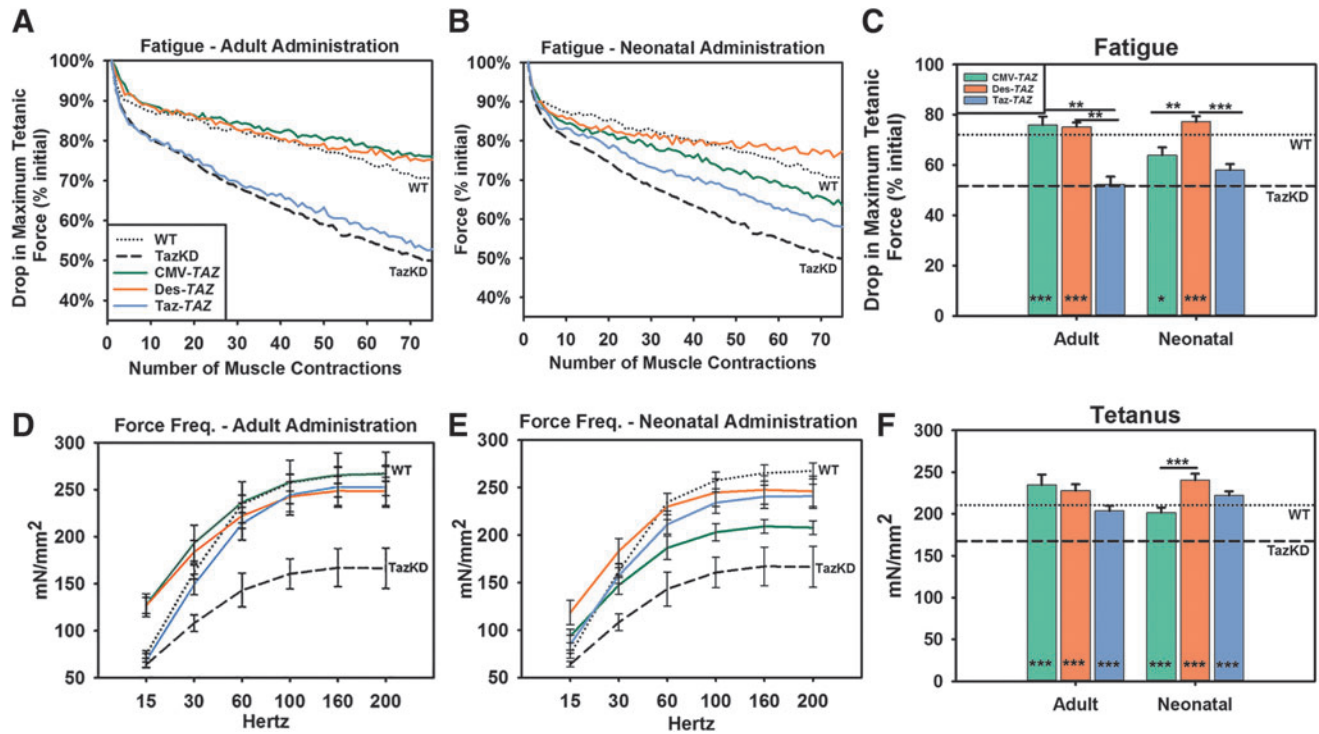


Figure 5. *Ex vivo* soleus muscle fatigue and strength force mechanics data. **(A, B)** Increased fatigability is observed in TazKD mice (dashed line) as compared with WT controls (dotted line) based upon comparisons of maximum tetanic force drop profiles of soleus muscles ($p \leq 0.001$). **(C)** Fatigability is significantly improved in all treatment cohorts except for those treated with the Taz-TAZ vector as either adults or neonates with differences between promoters indicated. **(D, E)** Soleus muscle strength based upon force frequency measurements is also significantly reduced in TazKD mice compared with WT controls ($p \leq 0.01$). **(F)** Soleus muscle strength based upon peak isometric tetanic force is increased in all treatment cohorts with differences between promoters indicated. Data are represented as mean \pm SEM ($n=6$). Significant differences between promoters for each treatment age are indicated by lines above bars and significant improvement between each individual sample and untreated TazKD controls is indicated at the bottom of bars (* $p \leq 0.05$, ** $p \leq 0.01$, *** $p \leq 0.001$).

(Fig. 5A–C). Mice treated as adults with CMV-TAZ or Des-TAZ both showed significant improvement in fatigability (final value of maximum force presented as a percentage of initial force) over mice treated with Taz-TAZ (Fig. 5C). Mice treated with Des-TAZ as neonates showed significant improvement in fatigability over both the other promoters. All treatment groups displayed significantly higher tetanic contractile force as compared to untreated TazKD controls (Fig. 5D–F). Mice treated as neonates with Des-TAZ showed significant improvement in peak isometric tetanic force over mice treated with CMV-TAZ (Fig. 5F).

TAZ gene therapy improves mitochondrial structural defects

Electron micrographs (EM) of hearts from untreated TazKD, WT controls, and mice in all treatment cohorts were examined to evaluate mitochondrial structure. Dramatic differences in mitochondrial size, numbers, and cristae organization were observed in EM images from healthy WT and untreated TazKD controls (Fig. 6A and E). All EM images from mice treated as adults show mito-

chondria that appear improved with regards to organization along sarcomeres, general size, and mitochondrial numbers and mice treated with either CMV-TAZ or Des-TAZ display improved cristae organization (Fig. 6B–D). All EM images from mice treated as neonates show mitochondria that appear improved with regards to decreased clustering between sarcomeres, general size, and cristae organization (Fig. 6F–G).

All treatment cohorts displayed significant improvements in mitochondrial area (increased relative to untreated TazKD controls) with mice treated as adults with Des-TAZ and Taz-TAZ displaying significant improvements over those treated with CMV-TAZ, and Taz-TAZ mice treated as neonates showing significant improvements over both of the other promoters (Fig. 6I). All cohorts except for those treated with Des-TAZ as neonates showed significant improvement in number of mitochondria per field (decreased) as compared to untreated TazKD controls with CMV-TAZ and Taz-TAZ displaying significant improvement over Des-TAZ mice treated as neonates (Fig. 6J). All cohorts showed significant improvement in mitochondrial

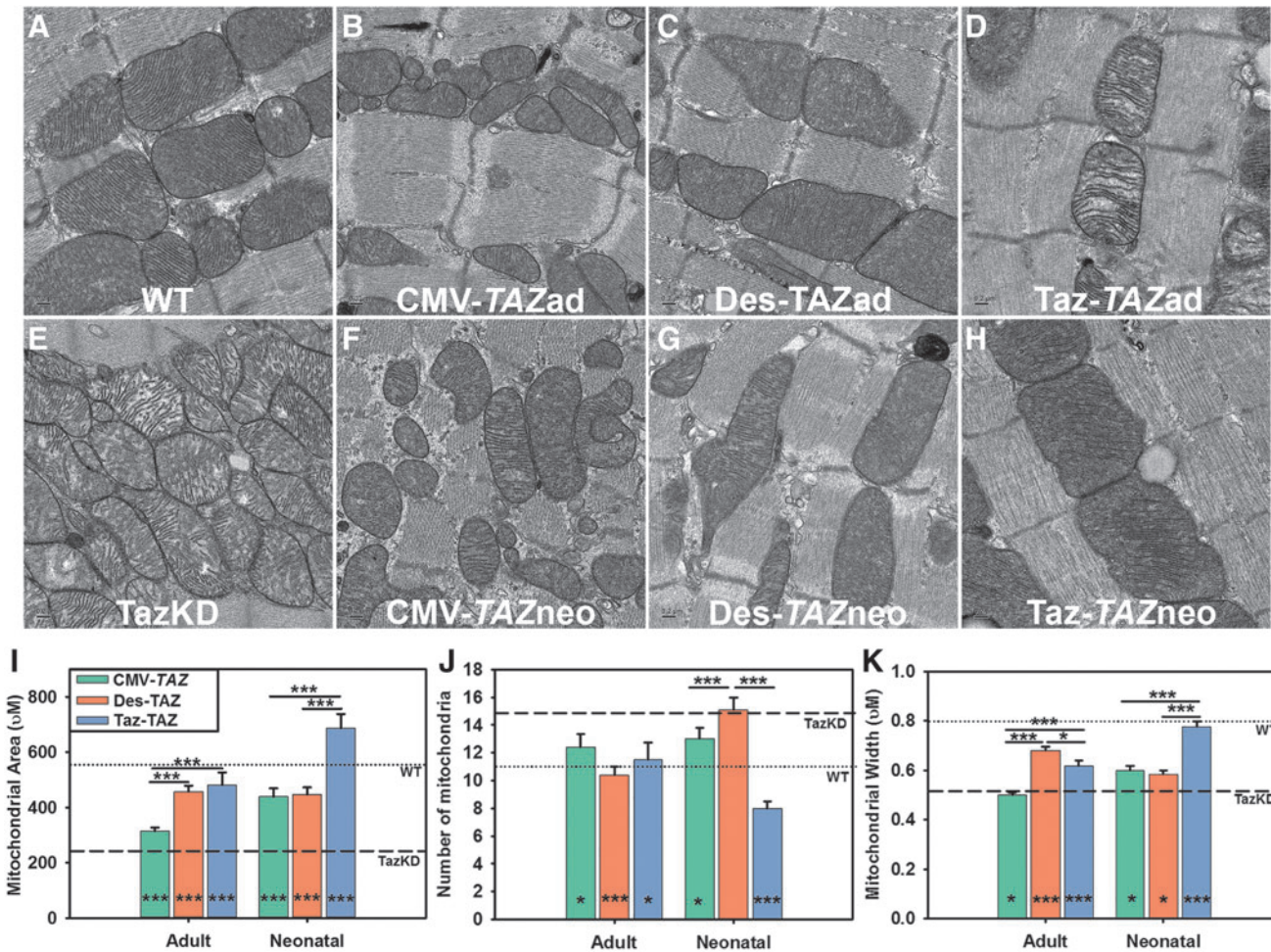


Figure 6. Mitochondrial structure evaluations. (A–H) Representative EM images of cardiac mitochondria from WT, TazKD, and all AAV treatment cohorts. Fifteen images from each of four samples were evaluated per group. (I–K) Quantitative evaluations of images (A–H) revealed significant differences between TazKD (dashed line) and WT (dotted line) mitochondrial area, number, and width ($***p \leq 0.001$). (I) Improved mitochondrial area was observed in all treatment cohorts. (J) Improved number of mitochondria per field was observed in every cohort except for Des-TAZ mice treated as neonates. (K) Improved mitochondrial width was observed in every cohort. Data are represented as mean \pm SEM. Significant differences between promoters for each treatment age are indicated by lines above bars and significant improvement between each individual sample and untreated TazKD controls is indicated at the bottom of bars ($*p \leq 0.05$, $**p \leq 0.01$, $***p \leq 0.001$).

width (increased) as compared to untreated TazKD controls with Taz-TAZ displaying significant improvement over CMV-TAZ and Des-TAZ displaying significant improvement over both other promoters in mice treated as adults (Fig. 6K). Mice treated with Taz-TAZ as neonates displayed a significant improvement in mitochondrial width as compared with both other promoters. In general, these EM images suggest that improved inner mitochondrial membrane organization, mitochondrial localization along sarcomeres, and a reduction in mitochondrial fragmentation is occurring in the hearts of treated mice.

TAZ gene therapy improves cardiac mitochondrial respiration

Oxygen consumption measurements were performed on freshly isolated, respiration competent,

cardiac mitochondria from mice at 5 months of age in all groups to examine differences in respiration states using an Oxytherm Clark electrode apparatus. Cardiac mitochondria from TazKD mice displayed significantly reduced levels of state 3 (mitochondria + glutamate/malate + ADP) O_2 consumption rates as compared with cardiac mitochondria isolated from healthy WT control mice (Fig. 7A). Significant improvements were observed in state 3 O_2 consumption rates from mice in all TazKD treatment groups as compared to untreated TazKD controls with no differences observed between promoters. Cardiac mitochondria from TazKD mice also displayed significantly reduced levels of state 4_o (ADP is depleted, oligomycin addition–ATP synthase inhibitor to prevent any contribution from ATP recycling in the ETC) O_2 consumption rates as compared with those iso-

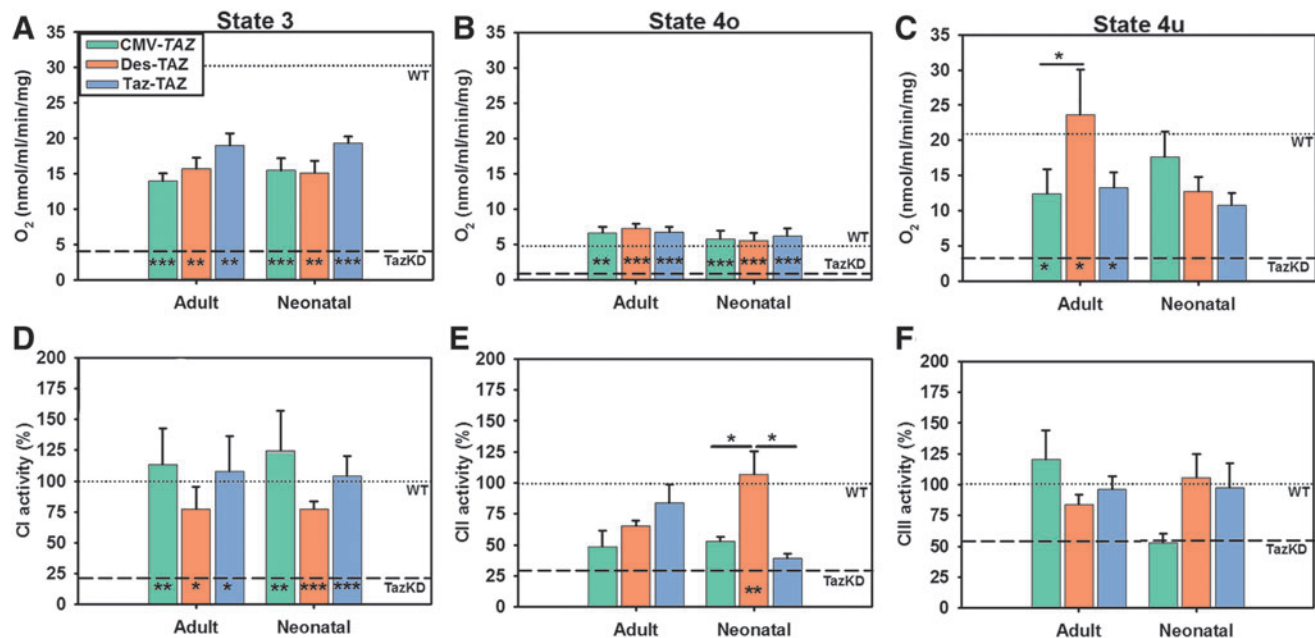


Figure 7. Cardiac mitochondrial function analyses: O₂ consumption and electron transport chain complex activities. A significant decrease in O₂ consumption rates state 3 (A), state 4_o [oligomycin added] (B), and state 4_u [uncoupled] (C) was observed in mitochondria isolated from the hearts of TazKD (dashed line) as compared to WT (dotted line) mice ($p \leq 0.001$). State 3 and state 4_o activities were significantly increased in mitochondria isolated from all treatment cohorts and state 4_u activity was significantly improved in the mice treated as adults. Cardiac mitochondrial complex I (CI), complex II (CII), and complex III (CIII) activities were evaluated and compared with WT (dotted line set at 100% activity). A significant decrease in activities was observed in TazKD (dashed line) compared with WT mice: CI ($p \leq 0.001$), CII ($p \leq 0.05$), CIII ($p \leq 0.05$). (D) All treated cohorts showed significant improvement in CI activity. (E) Only Des-TAZ mice treated as neonates displayed improvement in CII activity. (F) No treatment cohort displayed significant improvement in CIII activity levels. Data are represented as mean \pm SEM ($n=5$). Significant differences between promoters for each treatment age are indicated by lines above bars and significant improvement between each individual sample and untreated TazKD controls is indicated at the bottom of bars (* $p \leq 0.05$, ** $p \leq 0.01$, *** $p \leq 0.001$).

lated from healthy WT control mice (Fig. 7B). Significant improvements were found in state 4_o O₂ consumption rates from mice in all treatment groups as compared to untreated TazKD controls with no differences observed between promoters. Finally, cardiac mitochondria from TazKD mice displayed significantly reduced levels of state 4_u (FCCP added to uncouple electron transport and phosphorylation) O₂ consumption rates as compared to those isolated from healthy WT control mice (Fig. 7C). Significant improvements were found in all treatment groups with mice treated as adults with the Des-TAZ vector showing significant improvement over mice treated with CMV-TAZ. These respiration state data demonstrate an increased ability to consume oxygen in treated mitochondria which suggests more efficient ETC energy generation.

Mitochondrial ETC activities

Assays were performed to evaluate the activity levels of mitochondrial electron transport chain CI, CII, and CIII enzymes from lysates of isolated mitochondria. A significant decrease in CI, CII, and CIII activity levels was observed in TazKD mice as

compared to WT controls. CI activity levels were significantly improved in all treatment cohorts as compared to untreated TazKD controls and no differences were observed between promoters at either treatment age (Fig. 7D). CII levels were significantly improved in Des-TAZ mice treated as neonates as compared to untreated TazKD controls and CII activity in this cohort was significantly improved over both other promoters from the same injection age (Fig. 7E). CIII levels were not significantly improved in treated mice (Fig. 7F). These data provide further support that ETC energy generation is improved to some degree in all treatment cohorts.

Tabulated scores from all measurements

We developed a scoring system to determine which of the three promoters compared in this study (CMV, Des, or Taz) provided the highest number of desirable outcomes. Degree of significant improvement over untreated TazKD controls is indicated by the intensity of yellow shading (darker shading represents more significantly improved). Each box also indicates whether that vector and injection timepoint provide a result that is not significantly (ns) improved or is significantly

improved over one (+) or both (++) of the other two promoters. The tabulated scores (Table 1, bottom) show that Des-TAZ is the most optimal promoter for amelioration of overall BTHS pathophysiology, followed by CMV-TAZ, and finally, by Taz-TAZ regardless of gene therapy administration age.

DISCUSSION

As previous studies have demonstrated significantly impaired cardiac and skeletal muscle bioenergetics and exercise intolerance in BTHS-affected human patients, we sought to develop a gene therapy vector that would successfully treat both cardiac and skeletal muscle dysfunctions in BTHS.^{11,13} This study evaluated the *in vivo* performance of three different promoters within TAZ gene delivery vectors (CMV, Des, and Taz). We were particularly in-

terested identifying a promoter able to provide robust expression to cardiac and skeletal muscle with simultaneous low expression in the liver and other organs not impacted by BTHS as this would improve the safety and effectiveness of noninvasive intravenous gene therapy administration into human BTHS patients.

As the use of an AAV serotype with a high natural tropism for both cardiac and skeletal muscle is particularly advantageous for disorders such as BTHS, our study tested each of the three promoters packaged into AAV9 capsids. Due to a highly successful example of the use of AAV9 for spinal muscular atrophy 1 gene therapy, there is now a precedent for the safety and use of AAV9 as a clinical gene delivery vehicle.³⁹ Our experiments were performed using a well-established doxycycline-inducible shRNA knockdown mouse model of

Table 1. Barth syndrome gene therapy promoter comparison summary

Measurement (most desirable outcome)	CMVAd	DesAd	TazAd	CMVNeo	DesNeo	TazNeo
TAZ transcription (high in heart)	+	++	ns	ns	+	+
TAZ transcription (high in skeletal muscle—soleus)	ns	ns	ns	ns	++	ns
TAZ transcription (low in nonmuscle tissues—liver)	ns	ns	ns	ns	++	ns
TAZ translation (increased protein - WB)	ns	++	ns	ns	ns	ns
Pre-exercise activity - Resting time (decreased)	ns	ns	ns	ns	ns	ns
Pre-exercise activity - slow movement (decreased)	+	ns	ns	ns	ns	ns
Pre-exercise activity - fast movement (increased)	+	ns	ns	ns	ns	ns
Pre-exercise activity - average distance (increased)	ns	ns	ns	ns	ns	ns
Pre-exercise activity - rearing (increased)	ns	ns	ns	ns	++	ns
Post-exercise activity - resting time (decreased)	ns	ns	ns	+	+	ns
Post-exercise activity - slow movement (decreased)	ns	ns	ns	ns	++	ns
Post-exercise activity - fast movement (increased)	ns	ns	ns	+	++	ns
Post-exercise activity - average distance (increased)	ns	ns	ns	ns	++	ns
Post-exercise activity - rearing (increased)	ns	ns	ns	ns	+	ns
Echocardiography - ejection fraction (increased)	ns	ns	++	ns	ns	ns
Echocardiography - fractional shortening (increased)	ns	ns	++	ns	ns	ns
Heart weight/body weight ratios (decreased)	ns	ns	ns	ns	ns	ns
Force mechanics (decreased fatigability)	ns	+	ns	ns	+	ns
Force mechanics (increased strength)	ns	ns	ns	ns	+	ns
Mitochondrial number (decreased)	ns	ns	ns	+	ns	+
Mitochondrial area (increased)	ns	+	+	ns	ns	++
Mitochondrial width (increased)	ns	++	+	ns	ns	++
Mitochondrial oxygen consumption - state 3 (increased)	ns	ns	ns	ns	ns	ns
Mitochondrial oxygen consumption - state 4 _o (increased)	ns	ns	ns	ns	ns	ns
Mitochondrial oxygen consumption - state 4 _u (increased)	ns	+	ns	ns	ns	ns
Mitochondrial complex I activity (increased)	ns	ns	ns	ns	ns	ns
Mitochondrial complex II activity (increased)	ns	ns	ns	ns	++	ns
Mitochondrial complex III activity (increased)	ns	ns	ns	ns	ns	ns
Significant improvement over one other promoter within the same injection age (+). Total score:	3	3	2	3	5	2
Significant improvement over both other promoters within the same injection age (++) Total score:	0	3	2	0	7	2
Measurements significantly improved as compared to untreated TazKD ($p \leq 0.05$). Total score:	6	5	5	5	2	7
Measurements significantly improved as compared to untreated TazKD ($p \leq 0.01$) Total score:	8	7	7	6	10	4
Measurements significantly improved as compared to untreated TazKD ($p \leq 0.001$) Total score:	10	12	8	10	13	9
Sum of all improved outcomes:	27	30	24	24	37	24

All measurements conducted in this study are listed in the column on the left, with the most desirable outcome indicated in parentheses. The six columns to the right correspond to each promoter and age of treatment described in the study. The yellow shading indicates a direct comparison of how significantly improved that measurement is over untreated TazKD controls (dark yellow, $p \leq 0.001$; medium yellow, $p \leq 0.01$; and light yellow, $p \leq 0.05$). The significance of outcomes as compared with the other promoters is indicated for every measurement under each cohort with either ns (no significant improvement with this promoter over either of the other promoters), + (significant improvement with this promoter over one of the other promoters), or ++ (significant improvement with this promoter over both other promoters) at that same age of administration. The bottom of the table provides a summary breakdown score quantifying significance indicators for each treatment group, with total sums presented in the bottom row. WB, Western blotting.

BTHS. All mice were maintained on a dox diet throughout the study to control for any possible effects from doxycycline alone. We did not detect any effect of dox on AAV distribution as the overall vector distributions observed in our study were comparable to those profiles observed in other AAV9 characterization studies performed in mice without doxycycline.^{18,19,23} Some mice were treated as neonates (1–2 days) while others were treated as adults (3 months) to determine whether a different promoter would be more optimal for a particular age of treatment and confirm that a gene delivery approach is relevant for both infants and young men with BTHS.

While all three promoters provided substantial *TAZ* expression, the Des promoter provided the most optimal *TAZ* transcription level profiles with significantly higher expression in heart (both treatment ages) and skeletal muscle (neonatal administration), and significantly lower expression in liver (neonatal administration) as compared with the other two promoters. As expected, the CMV promoter demonstrated strong transcript expression levels across a variety of tissues and generally good functional improvement. However, it resulted in lower cardiac and higher liver expression than the Des promoter. By comparison, the *Taz* promoter displayed relatively low expression levels in the heart when delivered to adult mice, relatively high expression levels in the liver when delivered to neonates and resulted in the least overall functional improvement. Although BTHS primarily affects heart and skeletal muscle, tafazzin is normally expressed at low levels in many different tissues throughout the body; thus, the wide distribution of transcript expression generated from this native sequence is not entirely surprising.⁴⁰ Assessments of protein expression levels in the heart revealed improvement in most treated cohorts as compared to untreated controls. As anticipated based upon RNA transcript data, Des-*TAZ* administration to adult mice resulted in the highest levels based on both myc-tag pulldown and direct WB on whole-heart lysates.

Cardiac function, muscle strength, and exercise tolerance are all key features of BTHS that contribute to morbidity, mortality, and overall quality of life for these patients.^{10–13,41} Therefore, it was important to ensure that our gene therapy strategy addressed the complete pathophysiology of BTHS. Significant improvement was observed in *in vivo* cardiac function and heart weight/body weight ratios in all treatment cohorts as compared to untreated controls. O₂ consumption in isolated respiration competent cardiac mitochon-

dria and mitochondrial area were also significantly improved in all treatment cohorts as compared to untreated *TazKD* controls suggesting that achieving a modest increase in *TAZ* expression can have a dramatic impact on heart function in BTHS.

In vivo mouse activity and fatigability assessments (ActiTrack) demonstrated the ability of our gene therapy strategy to successfully improve whole body function. While differences between individual promoters were observed in several of these measurements, both the CMV-*TAZ* and Des-*TAZ* vectors demonstrated significant improvement over untreated controls in all ActiTrack assessments. Administration of the Des-*TAZ* vector to neonates resulted in statistically significant improvement (decreased fatigue) as compared with both other promoters in postexercise evaluations of slow movement time, fast movement time, and average distance travelled. Indeed, several treatment cohorts showed increased activity as compared with WT mice, which suggests that increased *TAZ* expression in muscle can increase mitochondrial energy production and dramatically improve function. Future overexpression studies to evaluate the impact of tafazzin overexpression in WT mice would confirm this and may mimic the results of previous mouse muscle exercise evaluations where metabolic adaptations improved mitochondrial function.^{42,43} Results from our *ex vivo* force mechanics assessments provide further support that *TAZ* gene delivery has the ability to improve strength and fatigability in BTHS. Together, our data suggest that increased *TAZ* expression in skeletal muscle can provide a key functional enhancement that will greatly improve quality of life for BTHS patients. As previous clinical studies demonstrated clear evidence for increased muscle fatigue in human BTHS patients due to inefficient O₂ utilization, an improvement in this parameter represents an important outcome measure for these patients.^{11,13}

If considered alone, any one of these vectors would appear beneficial as a therapy for BTHS. The direct comparison of three different therapeutic vectors presented in this study provides a basis for comparison that enables selection of the vector that is truly most optimal for translation into the clinic. In order to more easily visualize and consider how these promoters performed against one another, each vector's performance for every measurement included in the study was scored and tabulated. This approach identified the Des-*TAZ* vector as being the most prominently effective in BTHS mice treated as either adults or neonates

due to its overall ability to provide improvement to organelle, organ, and whole body function.

Future investigations will include development and testing of a Des-*TAZ* vector that has been codon optimized for transcription in humans as well as dose escalation studies in mice to more precisely estimate the optimal amount of vector required for a minimum effective dose and toxicology studies to ensure vector safety. In sum, we present the first demonstration of a potential definitive treatment that significantly improves heart and skeletal muscle function in BTHS whether delivered to very young or fully grown mice. Importantly, no negative effects were observed in any of the mice exposed to this therapeutic strategy. As a multitude of AAV-mediated gene delivery strategies are currently being evaluated for clinical efficacy in humans to treat a range of genetically inherited disorders (spinal muscular atrophy, hemophilia), a strong precedent exists for our strategy to be successfully implemented as a valid therapy.^{39,44} Thus, our study provides substantial support for the translation of dsAAV9-Des-*TAZ* gene therapy for BTHS into the clinical realm.

ACKNOWLEDGMENTS

The Barth Syndrome Foundation: Association Barth France and the Will McCurdy Fund for the Advancement of Therapies for Barth Syndrome (AGR DTD 03-06-2015; C.A.P.); Barth Syndrome Foundation of Canada (AGR DTD 7-14-2017; C.A.P.); the American Heart Association-Scientist Development (Grant No. 17SDG33410467; C.A.P.); the Children's Miracle Network: University of Florida Pediatrics Pilot Project (C.A.P.); the National Institutes of Health (R01 HL136759-01A1; C.A.P.); and National Institutes of Health (R01 HL107406-01A1; W.T.C.) all provided funding support for this study. We would also like to acknowledge Dr. Xiao Xiao (University of North Carolina) for sharing the dsAAV vector, the University of Florida Vector Core facility for AAV production, and the Emory University Robert P. Apkarian Integrated Microscopy Core for EM processing and imaging.

AUTHOR DISCLOSURE

No competing financial interests exist.

REFERENCES

1. Neuwald AF. Barth syndrome may be due to an acyltransferase deficiency. *Curr Biol* 1997;7:R465–466.
2. Houtkooper RH, Turkenburg M, Poll-The BT, Karall D, Pérez-Cerdá C, Morrone A, et al. The enigmatic role of tafazzin in cardiolipin metabolism. *Biochim Biophys Acta* 2009;1788:2003–2014.
3. Saini-Chohan HK, Holmes MG, Chicco AJ, Taylor WA, Moore RL, McCune SA, et al. Cardiolipin biosynthesis and remodeling enzymes are altered during development of heart failure. *J Lipid Res* 2009;50:1600–1608.
4. Valianpour F, Mitsakos V, Schlemmer D, Towbin JA, Taylor JM, Ekert PG, et al. Monolysocardiolipins accumulate in Barth syndrome but do not lead to enhanced apoptosis. *J Lipid Res* 2005;46:1182–1195.
5. Wang G, McCain ML, Yang L, He A, Pasqualini FS, Agarwal A, et al. Modeling the mitochondrial cardiomyopathy of Barth syndrome with induced pluripotent stem cell and heart-on-chip technologies. *Nat Med* 2014;20:616–623.
6. Schlame M. Cardiolipin synthesis for the assembly of bacterial and mitochondrial membranes. *J Lipid Res* 2008;49:1607–1620.
7. Xu Y, Kelley RI, Blanck TJ, Schlame M. Remodeling of cardiolipin by phospholipid transacylation. *J Biol Chem* 2003;278:51380–51385.
8. Schlame M, Ren M, Xu Y, Greenberg, ML, Haller I. Molecular symmetry in mitochondrial cardiolipins. *Chem Phys Lipids* 2005;138:38–49.
9. Schlame M, Kelley RI, Feigenbaum A, Towbin JA, Heerdt PM, Schieble T, et al. Phospholipid abnormalities in children with Barth syndrome. *J Am Coll Cardiol* 2003;42:1994–1999.
10. Spencer CT, Bryant RM, Day J, Gonzalez IL, Colan SD, Thompson WR, et al. Cardiac and clinical phenotype in Barth syndrome. *Pediatrics* 2006;118:e337–346.
11. Bashir A, Bohnert KL, Reeds DN, Peterson LR, Bittel AJ, de Las Fuentes L, et al. Impaired cardiac and skeletal muscle bioenergetics in children, adolescents, and young adults with Barth syndrome. *Physiol Rep* 2017;5:e13130.
12. Cade WT, Spencer CT, Reeds DN, Waggoner AD, O'Connor R, Maisenbacher M, et al. Substrate metabolism during basal and hyperinsulinemic conditions in adolescents and young-adults with Barth syndrome. *J Inherit Metab Dis* 2013;36:91–101.
13. Spencer CT, Byrne BJ, Bryant RM, Margossian R, Maisenbacher M, Breitenger P, et al. Impaired cardiac reserve and severely diminished skeletal muscle oxygen utilization mediate exercise intolerance in Barth syndrome. *Am J Physiol Heart Circ Physiol* 2011;301:H2122–H2129.
14. Vaz FM, Houtkooper RH, Valianpour F, Barth PG, Wanders RJ. Only one splice variant of the human TAZ gene encodes a functional protein with a role in cardiolipin metabolism. *J Biol Chem* 2003;278:43089–43094.
15. Xu Y, Zhang S, Malhotra A, Edelman-Novemsky I, Ma J, Kruppa A, et al. Characterization of tafazzin splice variants from humans and fruit flies. *J Biol Chem* 2009;284:29230–29239.
16. Khuchua Z, Yue Z, Batts L, Strauss AW. A zebrafish model of human Barth syndrome reveals the essential role of tafazzin in cardiac development and function. *Circ Res* 2006;99:201–208.
17. Schnepf BC, Clark KR, Klemanski DL, Pacak CA, Johnson PR. Genetic fate of recombinant adeno-associated virus vector genomes in muscle. *J Virol* 2003;77:3495–3504.
18. Inagaki K, Fuess S, Storm TA, Gibson GA, Mctiernan CF, Kay MA, et al. Robust systemic transduction with AAV9 vectors in mice: Efficient global cardiac gene transfer superior to that of AAV8. *Mol Ther* 2006;14:45–53.
19. Pacak CA, Mah CS, Thattaliyath BD, Conlon TJ, Lewis MA, Cloutier DE, et al. Recombinant adeno-associated virus serotype 9 leads to preferential cardiac transduction in vivo. *Circ Res* 2006;99:e3–9.

20. Zincarelli C, Soltys S, Rengo G, Rabinowitz JE. Analysis of AAV serotypes 1–9 mediated gene expression and tropism in mice after systemic injection. *Mol Ther* 2008;16:1073–1080.
21. Bish LT, Morine K, Sleeper MM, Sanmiguel J, Wu D, Gao G, et al. Adeno-associated virus (AAV) serotype 9 provides global cardiac gene transfer superior to AAV1, AAV6, AAV7, and AAV8 in the mouse and rat. *Hum Gene Ther* 2008;19:1359–1368.
22. Piras BA, Tian Y, Xu Y, Thomas NA, O'Connor DM, French BA, et al. Systemic injection of AAV9 carrying a periostin promoter targets gene expression to a myofibroblast-like lineage in mouse hearts after reperfused myocardial infarction. *Gene Ther* 2016;23:469–478.
23. Pacak CA, Sakai Y, Thattaliyath BD, Mah CS, Byrne BJ. Tissue specific promoters improve specificity of AAV9 mediated transgene expression following intra-vascular gene delivery in neonatal mice. *Genet Vaccines Ther* 2008;6:13.
24. Berneburg M. Research in practice: More than skin deep—aging of subcutaneous fat tissue. *J Dtsch Dermatol Ges* 2010;8:776–778.
25. Phoon CK, Acehan D, Schlame M, Stokes DL, Edelman-Novemsky I, Yu D, et al. Tafazzin knockdown in mice leads to a developmental cardiomyopathy with early diastolic dysfunction preceding myocardial noncompaction. *J Am Heart Assoc* 2012;1:e000455.
26. Soustek MS, Baligand C, Falk DJ, Walter GA, Lewin AS, Byrne BJ. Endurance training ameliorates complex 3 deficiency in a mouse model of Barth syndrome. *J Inherit Metab Dis* 2015;38:915–922.
27. Soustek MS, Falk DJ, Mah CS, Toth MJ, Schlame M, Lewin AS, et al. Characterization of a transgenic short hairpin RNA-induced murine model of Tafazzin deficiency. *Hum Gene Ther* 2011;22:865–871.
28. Kiebish MA, Yang K, Liu X, Mancuso DJ, Guan S, Zhao Z, et al. Dysfunctional cardiac mitochondrial bioenergetic, lipidomic, and signaling in a murine model of Barth syndrome. *J Lipid Res* 2013;54:1312–1325.
29. Wang Z, Ma H, Li J, Sun L, Zhang J, Xiao X. Rapid and highly efficient transduction by double-stranded adeno-associated virus vectors in vitro and in vivo. *Gene Ther* 2003;10:2105–2111.
30. McLaughlin SK, Collis P, Hermonat PL, Muzyczka N. Adeno-associated virus general transduction vectors: analysis of proviral structures. *J Virol* 1988;62:1963–1973.
31. Wei JF, Wei FS, Samulski RJ, Barranger JA. Expression of the human glucocerebrosidase and arylsulfatase A genes in murine and patient primary fibroblasts transduced by an adeno-associated virus vector. *Gene Ther* 1994;1:261–268.
32. Alexander MS, Casar JC, Motohashi N, Vieira NM, Eisenberg I, Marshall JL, et al. MicroRNA-486-dependent modulation of DOCK3/PTEN/AKT signaling pathways improves muscular dystrophy-associated symptoms. *J Clin Invest* 2014;124:2651–2667.
33. Kobayashi YM, Rader EP, Crawford RW, Iyengar NK, Thedens DR, Faulkner JA, et al. Sarcolemma-localized nNOS is required to maintain activity after mild exercise. *Nature* 2008;456:511–515.
34. Saha M, Mitsuhashi S, Jones MD, Manko K, Reddy HM, Bruels CC, Cho KA, et al. Consequences of MEGF10 deficiency on myoblast function and Notch1 interactions. *Hum Mol Genet* 2017;26:2984–3000.
35. Preble JM, Pacak CA, Kondo H, MacKay AA, Cowan DB, McCully JD. Rapid isolation and purification of mitochondria for transplantation by tissue dissociation and differential filtration. *J Vis Exp* 2014;(91):e51682.
36. Spinazzi M, Casarin A, Pertegato V, Salviati L, Angelini C. Assessment of mitochondrial respiratory chain enzymatic activities on tissues and cultured cells. *Nat Protoc* 2012;7:1235–1246.
37. Zolotukhin S. Production of recombinant adeno-associated virus vectors. *Hum Gene Ther* 2005;16:551–557.
38. Falk DJ, Mah CS, Soustek MS, Lee KZ, Elmallah MK, Cloutier DA, et al. Intrapleural administration of AAV9 improves neural and cardiorespiratory function in Pompe disease. *Mol Ther* 2013;21:1661–1667.
39. Mendell JR, Al-Zaidy S, Shell R, Arnold WD, Rodino-Klapac LR, Prior TW, et al. Single-dose gene-replacement therapy for spinal muscular atrophy. *N Engl J Med* 2017;377:1713–1722.
40. Fagerberg L, Hallström BM, Oksvold P, Kampf C, Djureinovic D, Odeberg J, et al. Analysis of the human tissue-specific expression by genome-wide integration of transcriptomics and antibody-based proteomics. *Mol Cell Proteomics* 2014;13:397–406.
41. Kraemer KH, DiGiovanna JJ, Moshell AN, Tarone RE, Peck GL. Prevention of skin cancer in xeroderma pigmentosum with the use of oral isotretinoin. *N Engl J Med* 1988;318:1633–1637.
42. Geng T, Li P, Okutsu M, Yin X, Kwek J, Zhang M, Yan Z. PGC-1alpha plays a functional role in exercise-induced mitochondrial biogenesis and angiogenesis but not fiber-type transformation in mouse skeletal muscle. *Am J Physiol Cell Physiol* 2010;298:C572–579.
43. Safdar A, Bourgeois JM, Ogborn DI, Little JP, Hettinga BP, Akhtar M, et al. Endurance exercise rescues progeroid aging and induces systemic mitochondrial rejuvenation in mtDNA mutator mice. *Proc Natl Acad Sci U S A* 2011;108:4135–4140.
44. George LA, Sullivan SK, Giermasz A, Rasko JEJ, Samelson-Jones BJ, Ducore J, et al. Hemophilia B gene therapy with a high-specificity factor IX variant. *N Engl J Med* 2017;377:2215–2227.

Received for publication February 12, 2018;
accepted after revision July 27, 2018.

Published online: August 1, 2018.